Eureka Open Access Journals
Open Access | Peer Reviewed | International Journals | Multidisciplinary Areas
OPEN ACCESS JOURNALS

Eureka Journal of Physical and Chemical Research (EJPCR)

ISSN 2760-490X (Online) Volume 2, Issue 5, May 2026

https://eurekaoa.com/index.php/1

THE EFFECT OF FAST NEUTRON IRRADIATION ON HIGH-TEMPERATURE YBCO SUPERCONDUCTING TAPES

Malika Anvarovna Mussaeva
Ahmad Abdunabievich Shodiev
Institute of Nuclear Physics Uzbekistan Academy of Sciences,
Mirzo Ulugbek District, 100214 Tashkent, Uzbekistan
mussaeva@inp.uz; akhmadshodiyev@gmail.com

ABSTRACT

The effect of 14 MeV fast neutron irradiation with a fluence of 2.5×10^{12} n/cm^2 on the structural and electrical properties of YBCO-coated superconducting tapes was investigated using X-ray diffraction (XRD) and Hall effect measurements. Neutron irradiation induces nanoscale defects, leading to noticeable modifications in the phase structure of the multilayer tape. A decrease in the average crystallite size and interplanar spacing, along with an increase in lattice microstrain and dislocation density, was observed for all identified phases, indicating defect formation and atomic-scale disorder. Electrical transport measurements reveal pronounced irradiation-induced trapping effects in the temperature range of 200–325 K, characterized by nonmonotonic conductivity and carrier concentration behavior. Effective activation energies extracted from temperature-dependent conductivity analysis lie in the range of 0.32–0.38 eV, reflecting complex carrier localization and transport processes associated with radiation-induced defects. The observed magnetoresistance features around 160 K are consistent with defect states commonly associated with oxygen vacancies, whose

Eureka Open Access Journals
Open Access | Peer Reviewed | International Journals | Multidisciplinary Areas
Eureka Journal of Physical and Chemical Research (EJPCR)
ISSN 2760-490X (Online) Volume 2, Issue 5, May 2026

https://eurekaoa.com/index.php/1

redistribution is evidenced by changes in peak shape after irradiation. The temperature range of 240–270 K, typically linked to oxygen ordering and vacancy migration in YBCO, is found to be particularly sensitive to neutron irradiation, resulting in strong carrier localization and pronounced trapping-detrapping phenomena. Despite these irradiation-induced modifications in the normal state, the results indicate that YBCO-coated tapes exhibit a high degree of radiation tolerance, supporting their potential application in fusion reactors and other radiation-intensive environments.

Keywords: YBCO-coated conductors; fast neutron irradiation; radiation-induced defects; X-ray diffraction; Hall effect; vortex pinning.

1. INTRODUCTION

The introduction of nanoscaled secondary phases so-called artificial pinning centers (APC) in superconducting cuprate thin films is a conventional approach to enhance the in-field critical current density, J_c (B, T) [1]. There are two ways to generate APC – either adding chemical nanoparticles or generating nanosized defects by nuclear particles irradiation. Coated superconductor tapes are vital for fusion power plants, where magnet coils generate strong magnetic fields needed for hot plasma confinement and are exposed to intense fast neutron fluxes. High-temperature superconductors (HTS) based on $YBa_2Cu_3O_{7-x}$ (YBCO) microfilm, are particularly promising due to their superior performance at 65–77 K.

Fig. 1 a shows a schematic of a superconducting tape - a $YBa_2Cu_3O_{7-x}$ coated conductor with a complex multilayer architecture - along with an illustration of the crystal structure and the hole doping mechanism of YBCO. It also shows the direction of the neutron beam and vortices pinned at structure

Eureka Open Access Journals
Open Access | Peer Reviewed | International Journals | Multidisciplinary Areas
Eureka Journal of Physical and Chemical Research (EJPCR)
ISSN 2760-490X (Online) Volume 2, Issue 5, May 2026

https://eurekaoa.com/index.php/1

defects. YBCO tapes were irradiated with fast neutrons (>0.1 MeV) up to fluency of 3.9×10^{22} m^{-2} at the Atominstitut reactor, critical current (I_c) measured at 30 K in magnetic fields up to 15 T increased to the maximal value at an intermediate fluency due to generated (APCs) [3]. For the first time, YBCO films and commercial REBCO tapes were exposed to 14 MeV neutrons from the D-T fusion reaction at the ENEA-Frascati Neutron Generator to the moderate fluency of 1.2×10^{14} cm^{-2}, and no significant changes in HTS properties were observed post-irradiation [4]. The effects of fast neutron irradiation on critical current density (J_c) and microstructural characteristics of highly textured YBCO bulks prepared by powder melting process have been investigated. The results indicated that the critical temperature (T_c) decreased insignificantly after irradiation with 5 fluencies up to 6.1×10^{17} n/cm^2, and the J_c values increased monotonously with irradiation [5].

New scaling laws were proposed to describe the in-field performance of HTS at low and moderate magnetic fields, and 3D-dimensional representation of pinning force density dependence on magnetic field and magnetic critical current density J_c at 75.5 K in YBCO thin film shown in Fig.1 b [6]. Thus, the primary niche for these laws is superconducting wires and tapes for cables, fault current limiters, and transformers.

Eureka Open Access Journals
Open Access | Peer Reviewed | International Journals | Multidisciplinary Areas

Eureka Journal of Physical and Chemical Research (EJPCR)

ISSN 2760-490X (Online) Volume 2, Issue 5, May 2026

https://eurekaoa.com/index.php/1

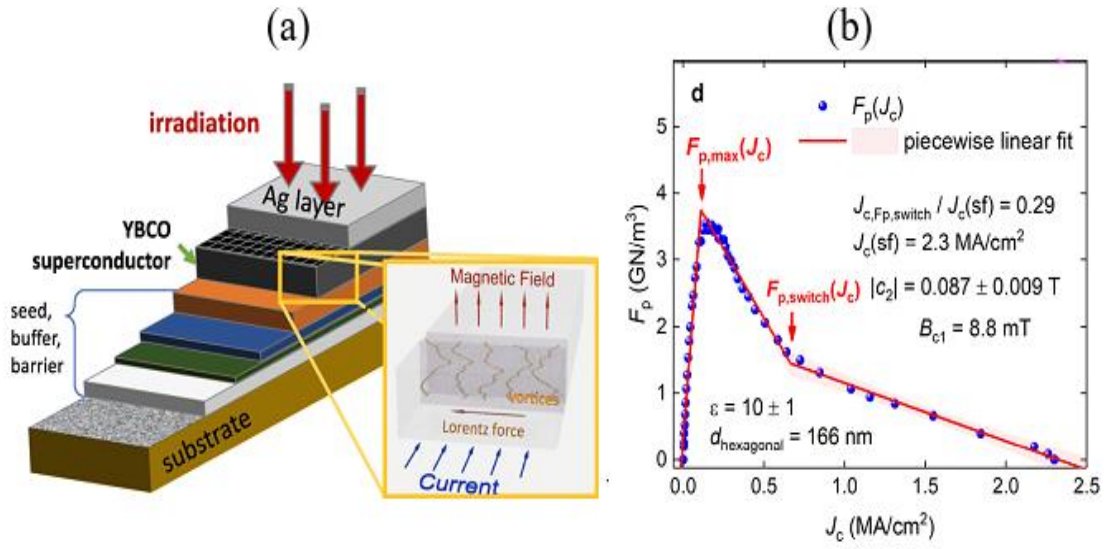

Fig. 1. (a) Schematics of a second-generation superconducting wire, an $YBa_2Cu_3O_{7-x}$ - coated conductor with complex multilayer architecture. These conductors were irradiated to improve critical currents. Inset shows vortex dynamics in superconductor with defects due to Lorentz forces [1–4, 9,10,12,13]. (b) Dependence of flux pinning force F_p on magnetic critical current density Jc in YBCO thin film at 75.5 K. The period of hexagonal vortice lattice d was calculated to be 166 nm at the indicated conditions [6]

The flux-pinning landscape in type-II superconductors determines the response of the flux line as shown in Fig.1a. If the changing magnetic field does not move the flux vortices from their pinning sites, their response remains linear and reversible. The vortex displacement, then, is characterized by the Campbell penetration depth, which itself is related directly to the effective size of the pinning potential [7]. The superconducting state originates from an enigmatic state called "strange metal" having a surprisingly simple linear temperature dependence of the resistivity, a possible

Eureka Open Access Journals
Open Access | Peer Reviewed | International Journals | Multidisciplinary Areas
Eureka Journal of Physical and Chemical Research (EJPCR)
ISSN 2760-490X (Online) Volume 2, Issue 5, May 2026

https://eurekaoa.com/index.php/1

consequence of the strong electron-electron correlations in these materials. This behavior cannot be accounted for by the conventional theories of electric transport and calls for new theoretical and experimental approaches.

The potential of neutron irradiation to enhance flux pinning and critical current density (J_c) in high-temperature superconductors has been extensively documented. For instance, Topal et al. [8] demonstrated that even at room temperature, irradiation with neutrons (E = 0.5 MeV, fluence $\Phi = 4.5\times10^{17}$ n/cm^2) leads to a sevenfold increase in J_c for $YBa_2Cu_3O_7$ and $SmBa_2Cu_3O_7$ superconductors at T = 50 K and B = 5 T. These results highlight the efficiency of radiation-induced defects as pinning centers, even when the irradiation is conducted at ambient temperatures, which aligns with the objectives of the present study on commercial YBCO tapes.

Aim of the Study. To investigate the effects of 14 MeV fast neutron irradiation and controlled oxygen reduction in $YBa_2Cu_3O_{7-x}$ HTS tapes, aiming to create lattice defects, optimize electron transfer from CuO chains to CuO_2 planes, enhance of the J_c value, and maintain or slightly increase in the T_c value within 80–95 K.

The study evaluates structural, electrical, and magnetic property changes, including phase composition, crystallite sizes, interplanar spacing, microstrain, dislocation density, conductivity, charge carrier mobility, magnetoresistance, and hall coefficient, to assess radiation tolerance for fusion reactors and high-radiation environments.

2. MATERIALS AND METHODS

Sample Preparation. We have used YBCO-based 4 mm wide coated conductor with a 5–8 μm thick superconducting layer manufactured by SuperPower in

Eureka Open Access Journals
Open Access | Peer Reviewed | International Journals | Multidisciplinary Areas
Eureka Journal of Physical and Chemical Research (EJPCR)
ISSN 2760-490X (Online) Volume 2, Issue 5, May 2026

https://eurekaoa.com/index.php/1

2011 on a 50 μm C276 steel substrate. The sequence of textured buffer layers from substrate to YBCO layer are Al_2O_3, Y_2O_3, MgO and $LaMnO_3$ using ion-beam assisted deposition (IBAD). After deposition of the YBCO superconducting layer using metal-organic chemical vapor deposition (MOCVD), the coated conductor was encased in Ag, Cu and PbSn [9].

To simulate fusion reactor operation conditions, the YBCO-coated tapes were exposed to 14 MeV monoenergetic fast neutrons produced by the NG-50 generator via the T (d, n) ^{4}He fusion reaction [11]. The irradiation was conducted in air at a temperature range of 290–310 K, reaching an integral fluence of 2.5×10^{12} n^o/cm^2. According to the technical specifications of d-T neutron generators, this setup ensures a nearly isotropic and monoenergetic neutron flux, minimizing spectral contamination [11]. The samples were positioned in a dedicated aluminum holder at a distance of 2–2.5 cm from the source to simulate the mechanical conditions of solenoid coils.

The microstructure and local element analysis of all microlayers of the received samples were examined before and after irradiations at SEM (EVO MA1O Zeiss) with installed EDS (energy dispersion system), both surface and lateral cut [12]. X-ray diffraction analysis was performed using a Panalytical Empyrean diffractometer in Bragg-Brentano geometry with CuKα radiation (λ = 0.15406 nm) as illustrated in Fig. 2 a.

Eureka Open Access Journals
Open Access | Peer Reviewed | International Journals | Multidisciplinary Areas

Eureka Journal of Physical and Chemical Research (EJPCR)

ISSN 2760-490X (Online) Volume 2, Issue 5, May 2026

https://eurekaoa.com/index.php/1

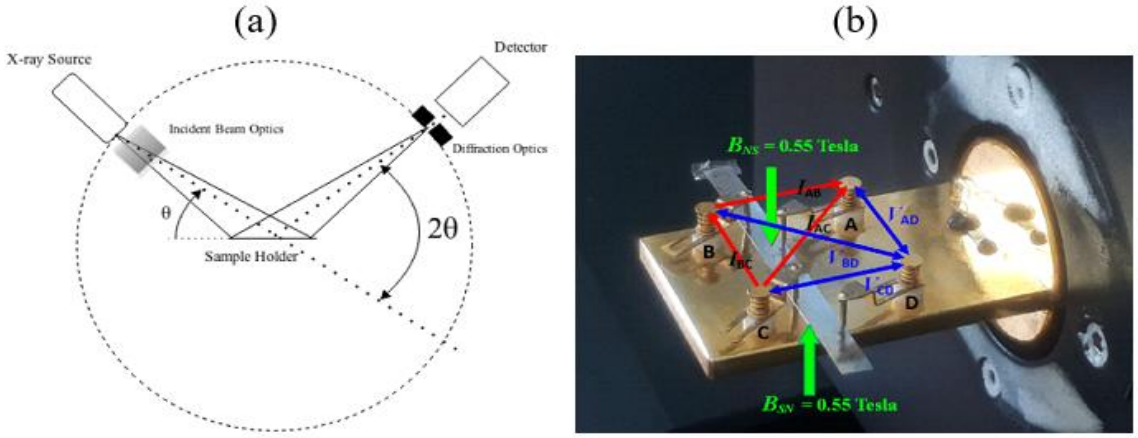

Fig. 2. (a) Schematic of X-ray diffractometer utilizing Bragg-Brentano geometry; (b) A measuring cell with 4 gold-plated contacts A-B-C-D pressing the sample, with arrows indicating the electric voltage V, magnetic field B of 0.55 Tesla, and current I

Measurements of X-ray intensity versus scattering angle (2θ) were recorded over the range $10° < 2\theta < 130°$. The HighScore Plus software package was employed for background fitting, peak profile analysis, and $K\alpha_2$ stripping. The c-axis lattice parameters were precisely determined through extrapolation to zero in a $\cos2\theta/\sin\theta$ plot derived from (00l) reflections, correcting for systematic errors caused by sample displacement from the diffractometer axis. Additionally, Williamson-Hall analysis was conducted to assess inhomogeneous strain within the sample [9]. The phase composition was determined using the PDF-2016 and COD databases.

The magnetic and electrical properties were measured using the four-point Hall effect method with an HMS-7000 system and an AMP55T magnet assembly (Ecopia, South Korea) in the temperature range of 80–350 K. The measurements were based on the Lorentz force and performed in the Van der

Eureka Open Access Journals
Open Access | Peer Reviewed | International Journals | Multidisciplinary Areas
Eureka Journal of Physical and Chemical Research (EJPCR)
ISSN 2760-490X (Online) Volume 2, Issue 5, May 2026

https://eurekaoa.com/index.php/1

Pauw configuration (Fig. 2 b). A tape sample 3.5 cm in length was mounted on the sample holder using four gold-plated contacts. The measurements were carried out in a magnetic field of B = 0.556 T with an applied current of I = 10 mA.

The magnetic and electrical characteristics of the SuperOx-1 tape, obtained through Hall effect measurements, as well as the XRD spectra collected by the diffractometer were processed and visualized using OriginPro 8 SR1 software.

2.1 XRD analysis and structural parameter calculation

Based on the X-ray diffraction (XRD) analysis, structural parameters were evaluated using the Scherrer equation, Bragg's law, and the Williamson-Hall (W-H) method.

The average crystallite size D was determined using the Scherrer formula (Eq. (1)).

$$D = \frac{K\lambda}{\beta \cos\theta} \quad (1)$$

The interplanar spacing d was calculated according to Bragg's law (Eq. (2)).

$$d_{hkl} = \frac{n\lambda}{2\sin\theta} \quad (2)$$

Lattice microstrain ε was estimated using the Williamson–Hall method within the framework of the uniform deformation model (UDM), considering the combined contributions of crystallite size and lattice strain to the diffraction peak broadening (Eq. (3)).

$$\varepsilon = \frac{\beta}{4\tan\theta} \quad (3)$$

Eureka Open Access Journals
Open Access | Peer Reviewed | International Journals | Multidisciplinary Areas
Eureka Journal of Physical and Chemical Research (EJPCR)
ISSN 2760-490X (Online) Volume 2, Issue 5, May 2026

https://eurekaoa.com/index.php/1

The dislocation density δ was calculated based on the crystallite size using Eq. (4).

$$\delta = \frac{1}{D^2} \quad (4)$$

Here, λ=0.15406 nm is the X-ray wavelength, β is the full width at half maximum (FWHM) of the diffraction peaks (in 2θ), θ is the Bragg diffraction angle, K=0.94 is the Scherrer constant, and D is the average crystallite size.

3. RESULTS AND DISCUSSION

3.1. Microstructure and morphology

Figure 3 shows a cross-sectional SEM image of the nonirradiated tape. While the overall multilayer architecture of the YBCO-coated superconducting tape is well preserved, significant variations in the thickness of the metal coating (Ag/Cu/PbSn) layers and the YBCO layer are observed.

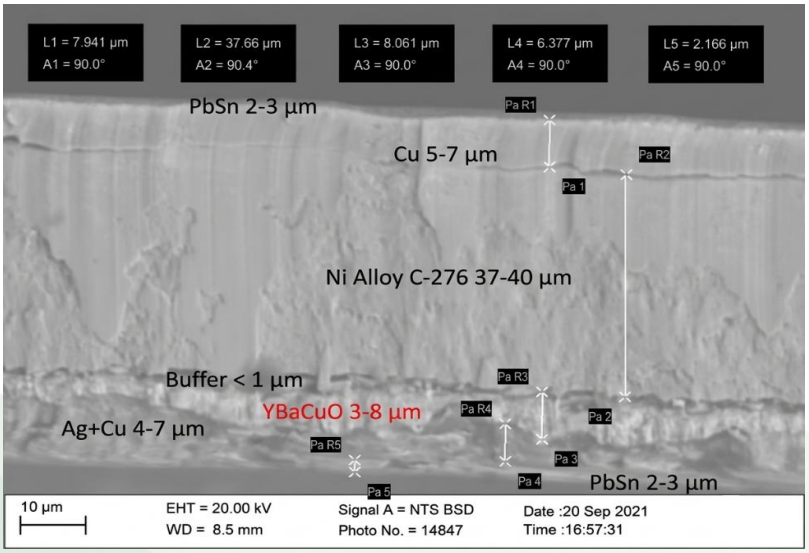

Fig. 1. SEM cross-sectional image of the YBCO-coated superconducting tape showing the multilayer architecture

Eureka Open Access Journals
Open Access | Peer Reviewed | International Journals | Multidisciplinary Areas
Eureka Journal of Physical and Chemical Research (EJPCR)
ISSN 2760-490X (Online) Volume 2, Issue 5, May 2026

https://eurekaoa.com/index.php/1

Such thickness non-uniformity is typical of industrially fabricated YBCO-coated superconducting tapes and should be considered when interpreting electrical transport and Hall effect measurements. This is because different local regions of the superconducting layer can contribute differently to the measured signals, particularly after irradiation with high-penetration particles, such as high-energy neutrons, which can efficiently induce defects.

3.2 Crystalline structure and phase composition

At first, available phases were identified (Fig.4, Table 1).

Table 1. Phase composition in % from XRD spectra

Pristine	$8Pb+6Sn+1Pb_{0.015}Sn_{0.985}+70Cu+8Ag+1CuO+3YBa_2Cu_2O_7+5Y_2O_3$
Irradiated	$4Pb+2Sn+6Pb_{0.015}Sn_{0.985}+64Cu+9Ag+3CuO+6YBa_2Cu_3O_7+6Y_2O_3$

As shown in Table 1, the pristine sample contains the primary HTS phase $YBa_2Cu_3O_7$ (T_c = 92 K) and an additional Y_2O_3 phase acting as artificial pinning centers (APC) [1], while the remaining phases correspond to technological coatings. After neutron irradiation, a noticeable increase in the peak area and intensity for the conductive YBCO and Y_2O_3 phases was observed, suggesting a radiation-induced structural rearrangement. This phenomenon, accompanied by the broadening of the diffraction peaks (FWHM), indicates the development of significant lattice microstrain and the formation of nanoscale defects within the superconducting layer.

Eureka Open Access Journals
Open Access | Peer Reviewed | International Journals | Multidisciplinary Areas
Eureka Journal of Physical and Chemical Research (EJPCR)
ISSN 2760-490X (Online) Volume 2, Issue 5, May 2026

https://eurekaoa.com/index.php/1

Based on X-ray diffraction (XRD) measurements performed before and after irradiation, the diffraction patterns of the YBCO tape were plotted using the OriginPro 2018 software. All identified diffraction peaks were subjected to detailed phase identification and structural analysis (Fig. 4). The results show that after irradiation the diffraction peaks exhibit a slight shift toward higher diffraction angles (to the right), accompanied by an increase in the full width at half maximum (FWHM). Since the tape consists of several functional layers, the irradiation-induced changes in the XRD patterns were analyzed by assigning the diffraction peaks to the corresponding phases of all layers. Structural parameters were then calculated for all identified peaks, and their average values were compared. The crystallite size (D) decreased from 49.73 nm to 36.42 nm, while the interplanar spacing (d) was reduced from 2.3636588 Å to 2.1484833 Å. At the same time, the lattice microstrain (ε) increased from 2.25×10^{-3} to 2.81×10^{-3}, and the dislocation density (δ) rose from 4.33×10^{-4} to 1.06×10^{-3}.

Based on the experimental measurements and calculated parameters, significant structural modifications are observed in the tape after neutron irradiation, indicating the formation of irradiation-induced defects. Similar studies have shown that such defects can act as effective pinning centers for Abrikosov vortices.

Eureka Open Access Journals
Open Access | Peer Reviewed | International Journals | Multidisciplinary Areas
Eureka Journal of Physical and Chemical Research (EJPCR)
ISSN 2760-490X (Online) Volume 2, Issue 5, May 2026

https://eurekaoa.com/index.php/1

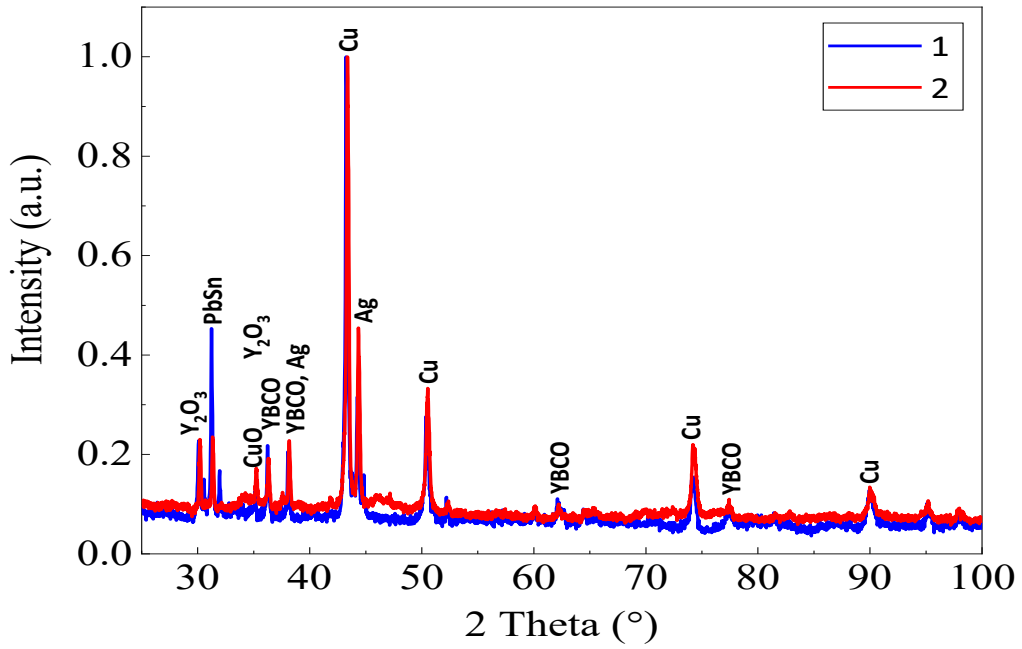

Fig. 4. XRD pattern (Intensity vs 2θ) of YBCO and corresponding structural parameters (D, d, ε, and δ) obtained from peak analysis. 1 – Reference, 2 – Irradiated integral fluence of 2.5×10^{12} n^o/cm^2 at an energy of 14 MeV

3.3 Hall Effect measurements and results

Figure 5 a shows the temperature dependence of the electrical conductivity σ for the pristine (curve 1) and neutron-irradiated (curve 2) YBCO tapes. For the pristine sample, the conductivity remains relatively stable over the entire measured temperature range, without pronounced anomalies.

Eureka Open Access Journals
Open Access | Peer Reviewed | International Journals | Multidisciplinary Areas

Eureka Journal of Physical and Chemical Research (EJPCR)

ISSN 2760-490X (Online) Volume 2, Issue 5, May 2026

https://eurekaoa.com/index.php/1

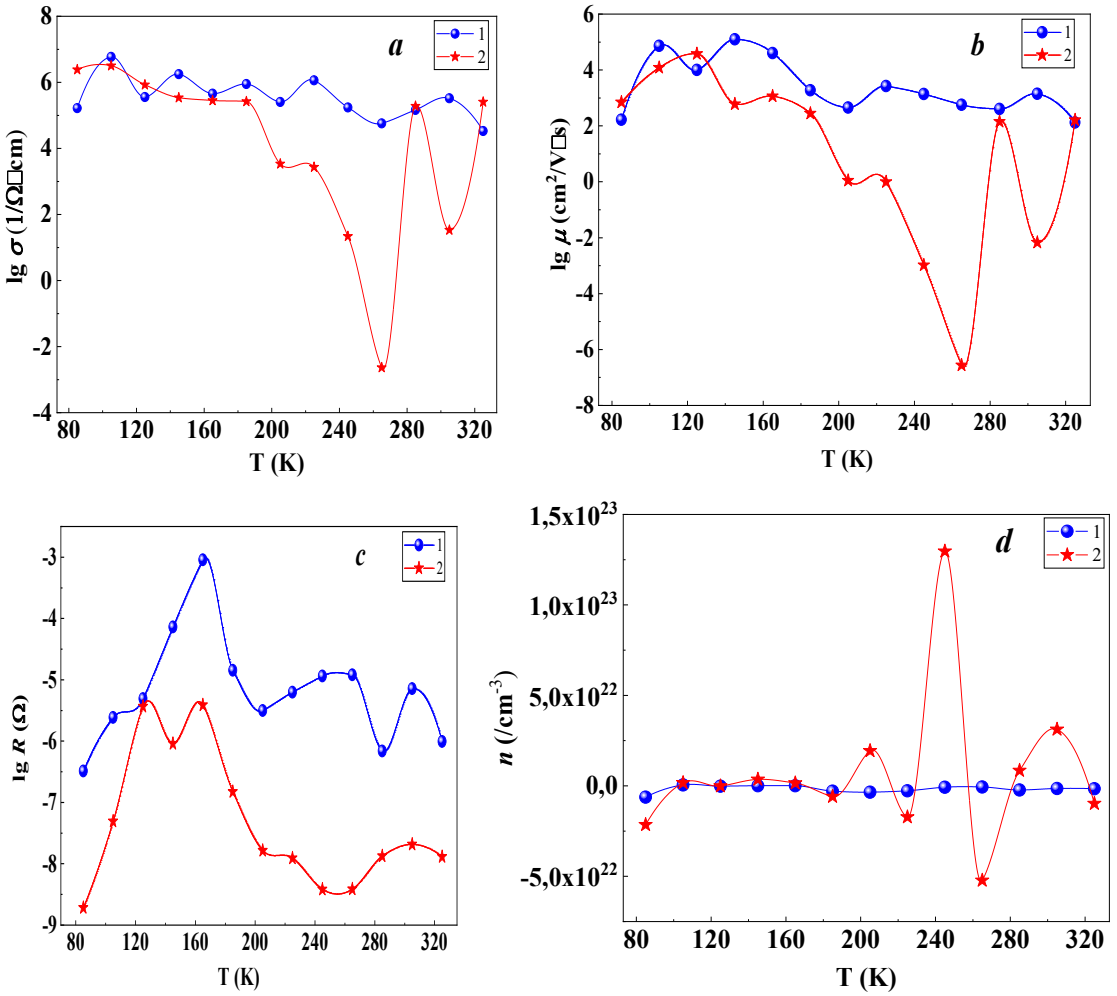

Fig. 5. Temperature-dependences of the conductivity (a), charge carrier mobility (b), magnetoresistance (c) and (d) charge carrier concentration measured in the Hall HMS-7000: 1 – pristine, 2 – tape irradiated at 300 K

This behavior indicates a low concentration of deep energetic traps and suggests that charge transport is mainly governed by intrinsic structural

Eureka Open Access Journals
Open Access | Peer Reviewed | International Journals | Multidisciplinary Areas
Eureka Journal of Physical and Chemical Research (EJPCR)
ISSN 2760-490X (Online) Volume 2, Issue 5, May 2026

https://eurekaoa.com/index.php/1

features of the YBCO tape. After fast neutron irradiation, the temperature dependence of σ changes significantly. In the temperature range of 200–320 K, pronounced anomalies accompanied by a sharp decrease in conductivity are observed. These features clearly indicate the formation of radiation-induced deep energetic states acting as charge carrier trapping centers. With increasing temperature, these traps become thermally activated in a stepwise manner, resulting in a complex and non-monotonic temperature dependence of the conductivity. The substantial difference between the pristine and irradiated curves reflects a significant increase in the density of defects and trapping centers induced by neutron irradiation. Within the framework of the thermally stimulated current (TSC) concept, the observed post-irradiation anomalies are associated with the presence of multiple radiation-induced defect levels characterized by different activation energies.

Within the first-order thermally stimulated current model (Eq. 5), the depths of the energetic traps were estimated from the temperatures corresponding to the maxima of the post-irradiation anomalies. The calculated trap energies are approximately 0.32 eV for the maximum near 285 K and about 0.38 eV for the maximum near 325 K, indicating the formation of shallow and intermediate radiation-induced defect states.

$$E_t = k_B T_m \ln\left(\frac{T_m^{\,2}}{\beta}\right) \qquad (5)$$

Here,

T_m – is the temperature of the TSC peak maximum (K),

β – is the heating rate (K/s), and

k_B – is the Boltzmann constant.

Eureka Open Access Journals
Open Access | Peer Reviewed | International Journals | Multidisciplinary Areas
Eureka Journal of Physical and Chemical Research (EJPCR)
ISSN 2760-490X (Online) Volume 2, Issue 5, May 2026

https://eurekaoa.com/index.php/1

Figure 5 b presents the temperature dependence of the charge carrier mobility. The most dramatic changes occur in the temperature range of 240–280 K. After irradiation (red curve), the mobility exhibits a sharp drop around 260 K, reaching strongly reduced and even anomalous values. This behavior indicates pronounced carrier localization caused by radiation-induced trapping.

This temperature range is particularly sensitive in YBCO, as 240–270 K is commonly associated with oxygen ordering processes and oxygen vacancy migration. Neutron irradiation disrupts this ordering, leading to the formation of deep and spatially complex trapping centers that strongly suppress carrier mobility.

Despite an increase in the charge carrier concentration after irradiation (Fig. 5 d), the strong reduction in mobility (Fig. 5 b) results in an overall decrease in electrical conductivity (Eq. 6). This clearly demonstrates that transport in the irradiated samples is limited primarily by carrier scattering and localization rather than by carrier availability.

$$\sigma = en\mu \qquad (6)$$

here:

e – electron charge (C)

n – concentration ($1/m^3$)

μ – mobility ($m^2/V\times s$)

The reduction of magnetoresistance after irradiation (Fig. 5 c, red curve) provides further evidence of irradiation-induced disorder. The increase in defect density introduces additional scattering centers and trapping sites within the YBCO lattice, modifying the classical relation $MR \propto (\mu B)^2$ through a strong suppression of carrier mobility. The peaks observed around 160 K are attributed to energetic levels associated with oxygen vacancies. Changes

Eureka Open Access Journals
Open Access | Peer Reviewed | International Journals | Multidisciplinary Areas
Eureka Journal of Physical and Chemical Research (EJPCR)
ISSN 2760-490X (Online) Volume 2, Issue 5, May 2026

https://eurekaoa.com/index.php/1

in the shape and intensity of these peaks after irradiation indicate a redistribution and increased complexity of defect configurations.

Figure 5 d shows the temperature dependence of the charge carrier concentration n(T) for both pristine and neutron-irradiated samples. For the pristine tape (curve 1), n(T) remains nearly constant over the entire temperature range, reflecting a stable electronic structure and the absence of significant trapping or detrapping processes.

In contrast, the irradiated sample (curve 2) exhibits strong fluctuations and pronounced extrema in the range of 200–300 K, including a sharp increase followed by a deep minimum. Such non-monotonic behavior is a clear signature of radiation-induced trapping and detrapping processes that strongly affect the effective carrier concentration. According to thermally stimulated current theory, these anomalies originate from the thermal release of carriers from localized defect states created by neutron irradiation. The coexistence of several (donor- and acceptor) types of trapping centers with different activation energies, along with possible recombination and re-trapping processes, leads to competing mechanisms of carrier release and loss. As a result, both positive and negative deviations in n(T) are observed.

In particular, since the sample is an industrial tape, it contains inherent defects, and the superconducting layer is not grown uniformly, as evidenced by the SEM cross-sectional image (Fig.3). Consequently, after irradiation, the defect density is lower in the thicker regions of the YBCO layer and higher in the thinner regions. In addition, during Hall effect measurements, it is difficult to determine whether the electrical contacts correspond to the thicker or thinner parts of the YBCO layer within the tape. Therefore, taking these aspects into account helps to better understand the underlying physical mechanisms and

Eureka Open Access Journals
Open Access | Peer Reviewed | International Journals | Multidisciplinary Areas
Eureka Journal of Physical and Chemical Research (EJPCR)
ISSN 2760-490X (Online) Volume 2, Issue 5, May 2026

https://eurekaoa.com/index.php/1

provides a more consistent explanation for the sharp variations observed in the Hall effect curves.

The strong contrast between the pristine and irradiated samples demonstrates that fast neutron irradiation significantly modifies the defect landscape and charge carrier dynamics in YBCO. While these radiation-induced defects deteriorate normal-state transport properties above T_c, they can serve as effective vortex pinning centers at temperatures below the superconducting transition.

4. CONCLUSIONS

The effect of 14 MeV fast neutron irradiation with a fluence of 2.5×10^{12} n/cm^2 on the structural and electrical transport properties of YBCO-coated superconducting tapes was investigated using X-ray diffraction and Hall effect measurements. XRD analysis revealed irradiation-induced structural disorder, evidenced by diffraction peak shifts toward higher angles, peak broadening, reduced crystallite size, and increased lattice microstrain and dislocation density, indicating the formation of nanoscale defects.

Electrical transport measurements showed that neutron irradiation strongly modifies the normal-state carrier dynamics. Pronounced nonmonotonic temperature dependences of conductivity, mobility, and carrier concentration were observed, reflecting radiation-induced trapping and detrapping processes. Effective activation energies of 0.32–0.38 eV were extracted, indicating complex carrier localization and transport mechanisms associated with irradiation-induced defects. Magnetoresistance anomalies, particularly around 160 K, are consistent with defect states related to oxygen vacancies and their redistribution after irradiation.

Eureka Open Access Journals
Open Access | Peer Reviewed | International Journals | Multidisciplinary Areas
Eureka Journal of Physical and Chemical Research (EJPCR)
ISSN 2760-490X (Online) Volume 2, Issue 5, May 2026

https://eurekaoa.com/index.php/1

Overall, the results demonstrate that fast neutron irradiation significantly alters the defect landscape and charge transport in YBCO-coated tapes. While irradiation degrades normal-state transport properties above T_c, the generated defects are expected to act as effective pinning centers for Abrikosov vortices, supporting the potential use of YBCO-coated conductors in radiation-intensive environments such as fusion reactors.

FUNDING

Acknowledgement. The authors are grateful to Dr. S.I. Tyutyunnikov and M.S. Novikov, PhD, from the Joint Institute for Nuclear Research, Dubna, Russian Federation, for providing the samples and supporting the research.
Special appreciation is extended to Professor E.M. Ibragimova for professional advice and constructive discussions; Professor S.V. Artemov and Engineer V. Tatarchuk for assistance with irradiation experiments; F. Khallokov, PhD, for support with X-ray analysis; and S. Egamov for help with Hall effect measurements.
The researches are supported by basic funding allocated to the Institute of Nuclear Physics of the Academy of Sciences of the Republic of Uzbekistan by the decree PP-4526.

Conflict of interest

The authors declare that they have no conflicts of interest.

Eureka Open Access Journals
Open Access | Peer Reviewed | International Journals | Multidisciplinary Areas
OPEN ACCESS JOURNALS

Eureka Journal of Physical and Chemical Research (EJPCR)

ISSN 2760-490X (Online) Volume 2, Issue 5, May 2026

https://eurekaoa.com/index.php/1

REFERENCES

1. Tsuchiya, K., Wang, X., Fujita, Sh., Ichinose, A., Yamada, K., Terashima, A., Kikuchi, A. "Superconducting properties of commercial REBCO-coated conductors with artificial pinning centers," Supercond. Sci. Technol., Vol. 34, p. 105005 (2021).
2. Antonova, L., Demikhov, T., Troitskii, A., Didyk, A. "Effect of 2.5 MeV proton irradiation on the critical parameters of composite HTS tapes," Phys. Status Solidi C, Vol. 12, No. 1–2, pp. 94–97 (2015). DOI: 10.1002/pssc.201400104
3. Fischer D. X, Prokopec R, Emhofer J, Eisterer M. The effect of fast neutron irradiation on the superconducting properties of REBCO coated conductors with and without artificial pinning centers // Supercond. Sci. Technol. 31. 044006 pp. 8 (2018). doi.10.1088/1361-6668/aaadf2
4. Pinto, V., Celentano, G., Angelis, De, M., Laviano, F., Masi, A., Pietropaolo, A., Tomellini, M., Torsello, D. "Effect of 14.1 MeV fusion neutron irradiation on YBCO thin films and commercial REBCO tapes," IEEE Trans. Appl. Supercond., Vol. 34, No. 3 (2024). DOI: 10.1109/TASC.2023.3337057
5. Zhang, P.X., Zhou, L., Bian, W.M., Ji, P., Wang, G., Wu, X.Z., Puzniak, R., Wisniewski, A., Baran, M., Szymczak, H. "Effects of fast neutron irradiation on Jc and microstructure of PMP-processed YBCO," Physica C, Vol. 282–287, pt. 3, pp. 1607–1608, (1997). DOI: 10.1016/S0921-4534(97)00887-3
6. Talantsev, E.F. "New Scaling Laws for Pinning Force Density in Superconductors," Condens. Matter, Vol. 7, p. 74, (2022). DOI: 10.3390/condmat7040074
7. Srpčič, J., Moseley, D., Perez, F., Huang, K.Y., Shi, Y., Dennis, A., Ainslie, M., Campbell, A., Boll, M., Cardwell, D., Durrell, J. "Flux vortex dynamics

Eureka Open Access Journals
Open Access | Peer Reviewed | International Journals | Multidisciplinary Areas
Eureka Journal of Physical and Chemical Research (EJPCR)
ISSN 2760-490X (Online) Volume 2, Issue 5, May 2026

https://eurekaoa.com/index.php/1

in type-II superconductors," Supercond. Sci. Technol., Vol. 33, p. 014003 (2020). DOI: 10.1088/1361-6668/ab5b53

8. Topal, U., Dorosinskii, L., Sozeri, H. Effect of neutron irradiation on pinning in SmBaCuO and YBaCuO superconductors. Physica C: Superconductivity, Vol. 407, No. 1–2, pp. 49-54, (2004). DOI: 10.1016/j.physc.2004.05.004
9. Nicholls, R.J., Diaz-Moreno, S., Iliffe, W., Linden, Y., Mousavi, T., Aramini, M., Danaie, M., Grovenor, C.R.M., Speller, S.C. Radiation-induced defects in high-temperature superconductors studied by high-energy X-ray spectroscopy. Communications Materials 3, 52 (2022).
10. Glatz, A., Sadovskyy, I., Welp, U., Kwok, W.K., Crabtree, G.W. "The quest for high critical current in applied high-temperature superconductors," J. Supercond. Nov. Magn., Vol. 33, pp. 127–141 (2020). DOI: 10.1007/s10948-019-05255-w
11. Neutron Generators for Analytical Purposes, IAEA Radiation Technology Reports No. 1, International Atomic Energy Agency, Vienna (2012).
12. Ibragimova, E.M., Shodiev, A.A., Ahrorova, S., Mussaeva, M.A., Iskandarov, N.E., Kurbanov, U.T., Tashmetov, M.Yu. "Low-dimensional magnetic centers in HTSC-YBCO film on steel-276 induced by gamma-quanta and electron beam," J. Magn. Magn. Mater., Vol. 595, p. 171617, (2024). DOI: 10.1016/j.jmmm.2023.171617
13. Ibragimova, E.M., Shodiev, A.A., Mussaeva, M.A., Yuldashev, B.S. "Magnetoresistance and carrier mobility in HTSC-YBCO tapes irradiated with 5 MeV electrons," Reports of the Academy of Sciences of the Republic of Uzbekistan, No. 1, pp. 33–39 (2024).